The time-course of spatiotopic updating across saccades

Authors

Jasper H. Fabius[1*], Alessio Fracasso[2,3,4], Tanja C.W. Nijboer[1,5] & Stefan Van der Stigchel[1]

Affiliations

[1] Experimental Psychology, Utrecht University, Utrecht, The Netherlands

[2] Institute of Neuroscience & Psychology, University of Glasgow, Glasgow, United Kingdom

[3] Radiology, Center for Image Sciences, University Medical Center Utrecht, Utrecht, The Netherlands

[4] Spinoza Center for Neuroimaging, University of Amsterdam, Amsterdam, The Netherlands

[5] Center of Excellence for Rehabilitation Medicine, Brain Center Rudolf Magnus, University Medical Center Utrecht, Utrecht University and De Hoogstraat Rehabilitation, Utrecht, the Netherlands

[*] Email: j.h.fabius@uu.nl

Author contributions

J.H.F., A.F. and S.S. conceived and designed experiments; J.H.F. performed experiments; J.H.F. analyzed data; J.H.F., A.F., T.C.W.N and S.S. wrote and revised the paper.

Additional information

This manuscript contains Supplemental Information. Experiment scripts, analysis scripts, and data are publicly available at Open Science Framework: DOI 10.17605/OSF.IO/HX5WP

Abstract

Humans move their eyes several times per second, yet we perceive the outside world as continuous despite the sudden disruptions created by each eye movement. To date, the mechanism that the brain employs to achieve visual continuity across eye movements remains unclear. While it has been proposed that the oculomotor system quickly updates and informs the visual system about the upcoming eye movement, behavioral studies investigating the time-course of this updating suggest the involvement of a slow mechanism, estimated to take more than 500 ms to operate effectively. This is a surprisingly slow estimate because both the visual system and the oculomotor system process information faster. If spatiotopic updating is indeed this slow, it cannot contribute to perceptual continuity because it is outside the temporal regime of typical oculomotor behavior. Here, we argue that the behavioral paradigms that have been used previously are suboptimal to measure the speed of spatiotopic updating. In this study, we used a fast gaze-contingent paradigm, using high phi as a continuous stimulus across eye movements. We observed fast spatiotopic updating within 150 ms after stimulus onset. The results suggest the involvement of a fast updating mechanism that predictively influences visual perception after an eye movement. The temporal characteristics of this mechanism are compatible with the rate at which saccadic eye movements are typically observed in natural viewing.

Significance statement

Humans make frequent eye movements – about 3-4 times per second. Eye movements create changes in sensory input that the visual system should dissociate from changes in the outside world. Still, visual perception is introspectively undisrupted, but appears continuous. It has been hypothesized that the visual system anticipates the sensory changes based on a predictive signal from the oculomotor system. However, psychophysical studies suggested that this anticipation develops slowly; too slow for natural vision. Here, we examined the speed of this anticipation more closely using psychophysics and a motion illusion. We observed fast anticipatory updating, quantifiable in human behavior. The time-scale at which the anticipation is reflected in behavior is compatible with typical fixation durations in natural viewing.

\body

Introduction

Humans sample the visual world by making fast, ballistic eye movements: saccades (1). Because acuity is not homogenous across the visual field (2), the fovea is directed to those locations that need to be inspected in closer detail. Saccades are made frequently – roughly every 200 to 300 ms (Fig. 1C; (3) – causing stimuli to fall on different locations on the retina several times per second. Still, feedforward processing of visual information in the brain is even faster – it is possible to decode stimulus specific representations within 100 ms after stimulus onset (4), and humans can discriminate a peripheral object and make a saccade towards it in 120 ms (5, 6). However, given that the visual system is largely retinotopically organized (7), saccades repeatedly create temporal discontinuities and spatial instabilities in the retinotopic representations, posing a problem for continuity in visual processing. Yet introspectively most humans perceive a continuous and stable visual world without these distortions generated by saccades.

How is perceptual continuity established? One prominent hypothesis is that the visual system anticipates the change in sensory input caused by a saccade based on a corollary discharge from the oculomotor system that carries information about the upcoming saccade (8, 9). Close to saccade onset, a subset of neurons respond to different retinotopic locations than they do under stable fixation (10–15). This anticipatory remapping of receptive fields could give rise to a transient non-retinotopic representation called *spatiotopic updating* (16, 17). Spatiotopic updating has been used to explain both the subjective impression of a continuous stream of visual perception across saccades (18, 19), as well as the objective psychophysical evidence for trans-saccadic integration of orientation, color, motion or higher-level features (20–33). In these studies, a pre-saccadic probe affected perception of a post-saccadic stimulus at the same spatiotopic location.

Because the oculomotor system executes about 3-4 saccades per second, spatiotopic updating should operate within a small time-window to facilitate perceptual continuity across saccades. Within a single fixation, pre-saccadic information should be updated and be available directly after the saccade. Concerning the post-saccadic availability, different experiments demonstrated that spatiotopic updating primarily affects perception immediately after saccades (20, 34–36). But concerning the pre-saccadic updating of visual information, spatiotopic representations have been estimated to develop surprisingly slow, requiring fixation durations of more than 500 ms (37–41). This raises a question: if visual processing is fast – content specific representations in 100 ms – and the saccade system is fast – 250 ms between two saccades – why is spatiotopic updating slow?

We hypothesized that the apparent slow speed of spatiotopic updating resulted from the nature and interpretation of the psychophysical tasks that have been used. The tilt aftereffect (TAE) is one such example (37, 38), although updating of the TAE is not without controversy (42, 43). The TAE is a perceptual aftereffect where the perceived orientation of a test stimulus is changed after prolonged exposure of another oriented grating, the adapter. When the test stimulus is presented with an orientation away from the adapter, perceptual reports tend to be even further away from the adapter (44). Because the TAE is a slow process – still increasing in magnitude after 10 minutes (45) – it might not be a particularly sensitive paradigm to investigate fast visual processing across saccades. To investigate spatiotopic updating, the TAE has been tested in a spatiotopic reference frame where a saccade was made between the presentation of the adapter and the test stimulus. The time-course of spatiotopic updating was inferred to take a long time because the TAE increases in strength when saccades were delayed. This increase continues for delays up to 1000 ms. Similar results were obtained for delayed saccades with saccadic suppression of intrasaccadic displacement (40) and perisaccadic mislocalization (41). However, although the effects were strongest for the longest delays, they were already apparent even for short delays. Finally, it should be noted that in most trans-saccadic experiments, like these with the TAE, two essentially different stimuli are presented before and after the saccade, violating the assumption of a stable, continuous visual world across the saccade. Indeed, psychophysical evidence shows that when visual stimuli are continuous across saccades, observers perceive the continuity, whereas if reliable intra-saccadic changes are made to the stimuli, observers expect stimuli to change during a saccade (46). To study visual continuity, the experimental stimulus should also be continuous (47).

To test spatiotopic updating within the time-window of 250 ms before saccade onset, we used our recently developed psychophysical, gaze-contingent paradigm (20) with a fast motion illusion: high phi (48). This paradigm allows for the examination of the complete time-course of spatiotopic updating. In high phi, subjects see an annulus with a random low-pass filtered texture. This annulus rotates slowly (*inducer*), after which its texture is sequentially replaced by four different random textures (*transient*). This creates an illusory transient percept of a large rotational step in the opposite direction from the preceding inducer. Previous experiments with high phi have shown that high phi can be experienced with inducers as brief as 50 ms (Fig. 1B). In our previous study, we observed that it is possible to induce the illusion in a spatiotopic reference frame, when testing with long inducer previews (>500 ms).

Here, we presented an inducer in the peripheral visual field *(inducer preview)* and asked subjects to make a saccade to the center of the inducer as soon as it appeared, i.e. visually guided saccades. After the saccade the inducer continued to rotate briefly (*post-saccadic inducer)*, followed by the *transient*. If the rotational motion of the inducer preview is spatiotopically updated across the saccade, the rotational information of the preview should be added to the rotational information of the post-saccadic inducer, resulting in stronger high phi. Alternatively, if the rotational motion of the inducer preview is not (yet) spatiotopically updated, the strength of high phi is only related to the post-saccadic inducer. To test whether spatiotopic updating can indeed be observed within the temporal regime of visually guided saccades (3), we kept the duration of the inducer preview as long as (Experiment 1) or shorter than (Experiment 2) the saccade latencies of our subjects. Thus, we were able to dissociate whether spatiotopic updating itself is slow, or whether updating occurs at a shorter time-scale but previous paradigms were not sensitive to this fast process.

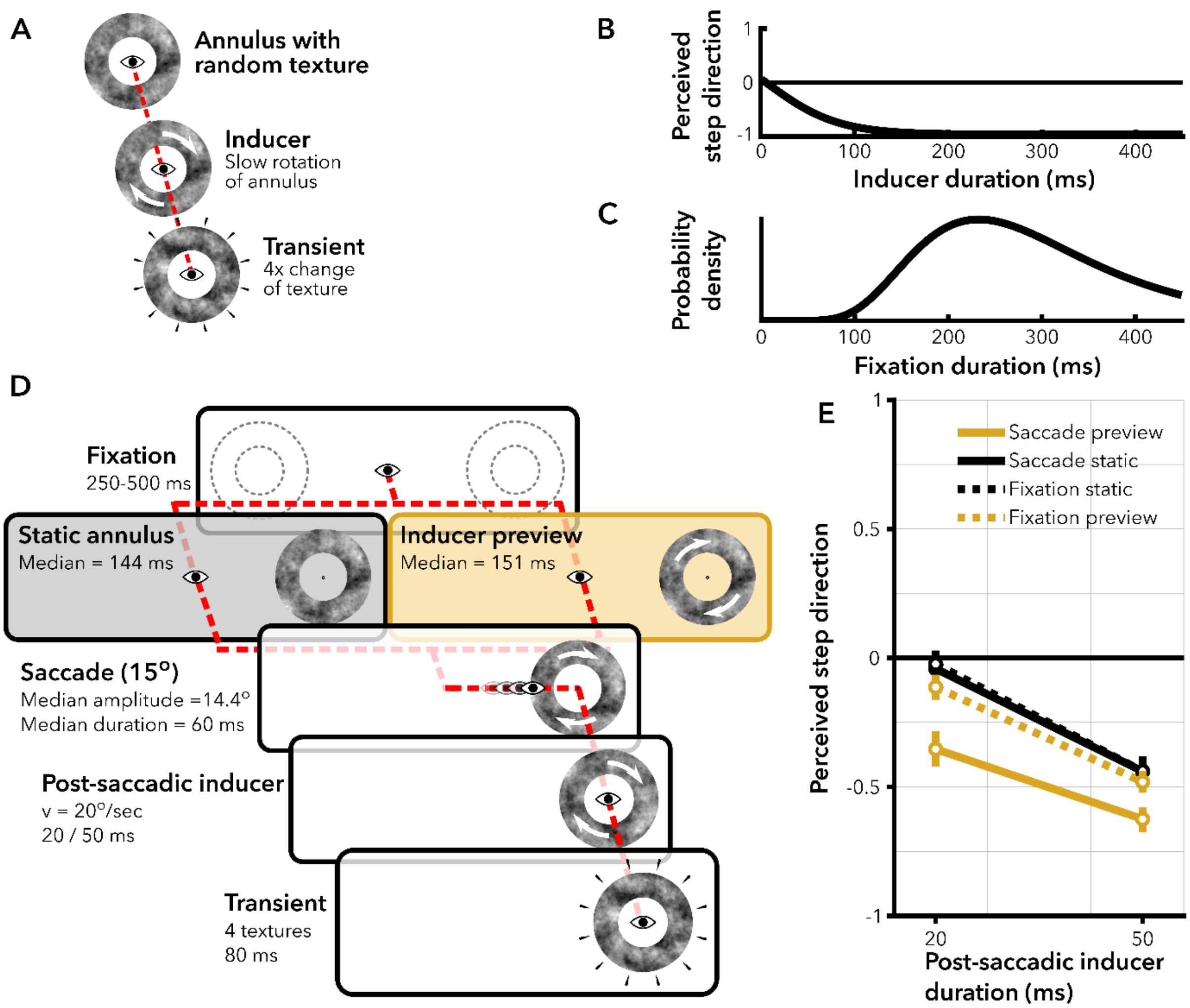

Figure 1. Experiment 1, design and results. **A)** High phi example (48). An annulus of random low-pass filter noise is presented around the point of fixation. The annulus starts rotating slowly (inducer), clockwise (CW) or counterclockwise (CCW). Then, the random noise texture is replaced rapidly by four different textures, 20 ms/texture (transient). The transient induces the percept of a large rotational step in the opposite direction from the inducer. The percept of a backward step is illusory because on average the

change of textures does not contain global motion in CW or CCW direction. **B)** Perceived step direction with high phi as a function of inducer duration. Observers indicate whether they perceived a CW or CCW step when the transient was presented. Their responses were recoded to forward (1) or backward (-1) with respect to the rotation direction of the preceding inducer. More negative numbers reflect a stronger bias to perceive backward steps, and thus a stronger high phi. High phi increases with longer inducers but is already apparent after brief inducers. **C)** Example distribution of fixation durations in natural viewing tasks (based on ref. (3). Comparing B and C, it can be noted that high phi can be induced within the temporal limits of a typical fixation. **D)** Gaze-contingent conditions in Experiment 1. The two conditions proceeded almost identically, with the only exception that the annulus remained static until saccade onset (Saccade static, black) or started rotating immediately upon onset (Saccade preview, yellow). Subjects maintained fixation until the annuli appeared. The dotted lines in the first panel were not actually visible but merely illustrate that the stimuli could appear at two locations (equal probability). The eye indicates gaze position in each panel. Arrows on the annuli illustrate that the annulus rotated in that phase of the trial. Median saccade parameters in row 2 and 3 were obtained from the trials that were included in the analysis. **E)** Model estimates of the average perceived step direction, where the error bars represent the 95%-CI of the estimates obtained with non-parametric bootstrapping.

Results

Rapid spatiotopic updating

In Experiment 1, we measured the strength of high phi in four conditions (see *SI Appendix)*, two trans-saccadic conditions (Fig. 1D) and two additional conditions where subjects maintained fixation to control for a spatial invariant effect (see next section *Control for spatially invariant effect*). The direct test for spatiotopic updating is the comparison between the two trans-saccadic conditions. In the *Saccade preview* condition, subjects were presented the inducer before saccade onset, whereas in the *Saccade static* condition, subjects were presented a static annulus before saccade onset. After the saccade the annulus rotated briefly for 20 or 50 ms in both conditions, followed by the transient. Subjects indicated whether they perceived a large clockwise or counterclockwise step. We analyzed responses with a logistic linear mixed effects model, with condition and post-saccadic inducer duration as fixed effects. The estimated intercept of the model gives the log odds of the transient being reported as a forward rotational step in the *Saccade preview* condition. The other estimated coefficients (β) are relative to this intercept (Fig. 3A). A negative coefficient indicates a higher probability of perceiving the transient as a backward rotational step.

Longer durations of the post-saccadic inducer lead to more frequent percepts of backward rotational steps (β = -0.36/10 ms, 95%-CI = [-0.41, -0.31], $F(1,7957) = 80.98$, $p < 0.001$). This shows that high phi rapidly increases in strength with longer inducers, similar to previous the results of previous experiments (20, 48). Importantly, if the inducer is previewed in the periphery before saccade execution (*Saccade preview*, Fig. 1E, yellow solid line), high phi is stronger than in the *Saccade static* condition after the saccade (Fig. 1E, black solid line; β = 0.63, 95%-CI = [0.33, 0.91], $F(1,7957) = 17.54$, $p = 0.001$). The preview effect can be interpreted as a spatiotopically transferred effect of the inducer preview: the visual system updated the location of the rotating inducer to a spatiotopic reference frame before the saccade. As a result, the inducer preview and the post-saccadic inducer jointly biased perception after the saccade, inducing a stronger high phi. We estimate that the preview resulted in an approximate 17.5 ms (95%-CI = [10.7, 27.3] ms) 'head start' in visual processing after saccades with latencies of 150 ms, by taking the ratio of the coefficient of the *Saccade static* condition (β = 0.63) and the coefficient of the post-saccadic inducer (β = -0.36/10 ms). This preview effect generalizes to annuli that cover different and more peripheral portions of the visual field (inner, outer radius = [2.6, 5.0]° and [6.0, 9.25]°), as observed in a control experiment with different subjects (*SI Appendix)*.

Control for spatially invariant effect

The observed spatiotopic preview effect could potentially be explained by a general, spatially invariant induction of high phi. Such an effect should also be observed without the execution of a saccade. Therefore, we measured high phi in two conditions without saccades, where subjects maintained fixation at the center of the screen and either an inducer (*Fixation preview*) or static annulus (*Fixation static*) was presented in the periphery before the annulus was presented around fixation (Fig. S1; *SI Appendix*). The results of the *Fixation preview* (Fig. 1E, yellow dashed line) condition demonstrate that a spatially invariant effect cannot fully account for the observed spatiotopic effect, because the illusion was less strong in the *Fixation preview* condition than in the *Saccade preview* condition ($\beta = 0.37$, 95%-CI = [0.11, 0.63]; $F(1,7957) = 10.13$, $p = 0.006$). However, high phi in the *Fixation preview* condition was slightly stronger than in the *Fixation static* (Fig. S1A) condition ($F(1,7957) = 7.85$, $p = 0.015$). In short, we observed a limited spatially invariant effect but this cannot fully account for the trans-saccadic preview effect.

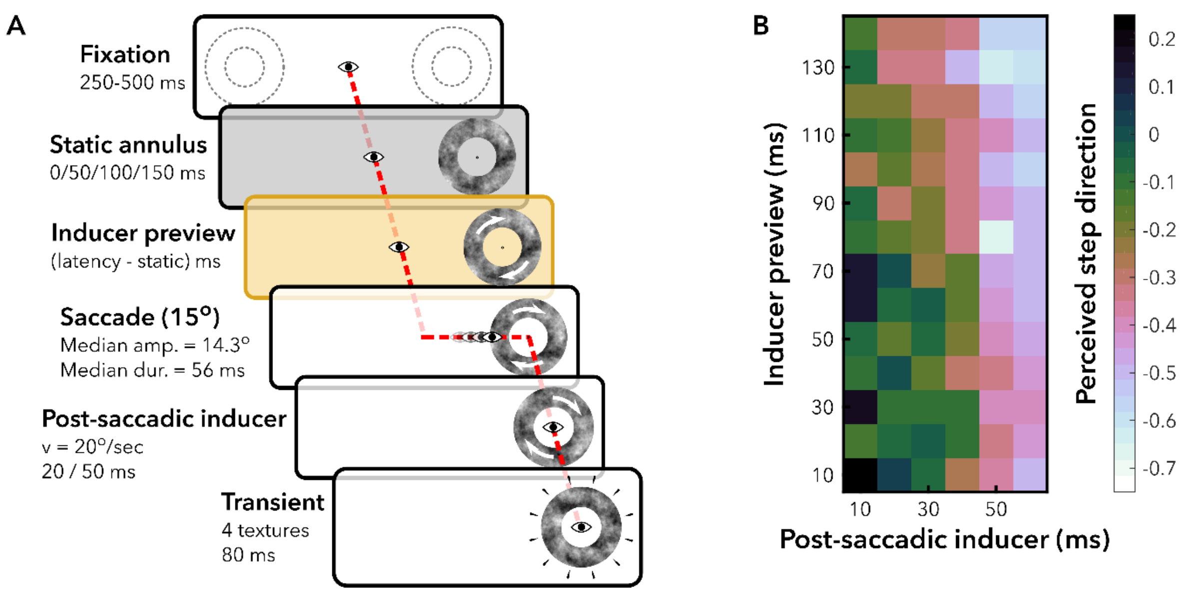

Figure 2. Experiment 2, design and results. **A)** Subjects fixated a fixation target for 250-500 ms. An annulus appeared in the periphery. The annulus remained static for 0, 50, 100 or 150 ms, and then started rotating. The annulus continued to rotate throughout the saccade and 20 or 50 ms after (post-saccadic inducer). If subjects moved their eyes before the annulus started rotating, it started rotating when gaze was detected >3º away from the fixation target. After the post-saccadic inducer, the texture of the annulus was replaced by 4 different, random textures (20 ms/texture). Subjects indicated whether they perceived the change in textures as a step in CW or CCW direction. Responses were recoded to 'backward' and 'forward' with respect to the rotation direction of the preceding inducer. **B)** Estimated perceived step direction from the mixed effects model as a function of inducer preview (y-axis) and post-saccadic inducer (x-axis) . Brighter colors indicate more frequent percepts of backward steps. The range of the colormap goes from 0.25 to -0.75 to optimize color contrasts for the range of plotted values.

Duration of pre-saccadic preview and strength of post-saccadic bias

In Experiment 1, the inducer preview biased post-saccadic perception of the same stimulus when it was presented in the same spatiotopic location. In general, the strength of high phi depends on inducer duration. We examined whether the strength of the preview effect similarly depends on preview duration. In Experiment 1, the duration of the inducer preview coincides with saccade latency. We constructed a second mixed effects model, using only data from the *Saccade preview* condition. Preview duration and post-saccadic inducer duration were fixed effects, and we included random effects per subject for the fixed effects and inducer rotation direction. We compared this model to a null-model without a fixed effect for preview duration. Preview duration did not improve the model fit ($\chi^2(1) = 0.82$, $p = 0.36$), so it seems that the preview effect was not modulated by preview duration. However, if the preview effect is perceptual in nature it should be related to the strength of the preview. To test the limits of the preview effect, in Experiment 2 we uncoupled preview duration and saccade latency for even shorter preview durations than in Experiment 1.

In Experiment 2, each preview consisted of a mixture of a static annulus followed by an inducer preview (Fig. 2A; *SI Appendix*). The data were analyzed with a mixed effects model, with fixed effects for preview duration and post-saccadic inducer duration; random effects per subject. The model with preview duration as a fixed effect was a better fit for the data than the model without it ($\chi^2(1) = 8.99$, $p = 0.003$). In this model, a longer preview duration results in more frequent percepts of a backward step (Fig. 2B; $\beta = -0.05$/10 ms, 95%-CI = [-0.07, -0.02], $F(1, 3799) = 13.99$, $p < 0.001$). In addition to the effect of the inducer preview, the post-saccadic inducer also induced a strong bias, similar to Experiment 1 ($\beta = -0.30$/10 ms, 95%-CI = [-0.35, -0.25], $F(1, 3799) = 91.90$, $p < 0.001$). The estimated coefficients are displayed in Fig. 3B. In sum, both in Experiment 1 and 2 we observed spatiotopic updating within 150 ms after stimulus onset. Moreover, the duration of the preview increases the strength of the spatiotopic effect.

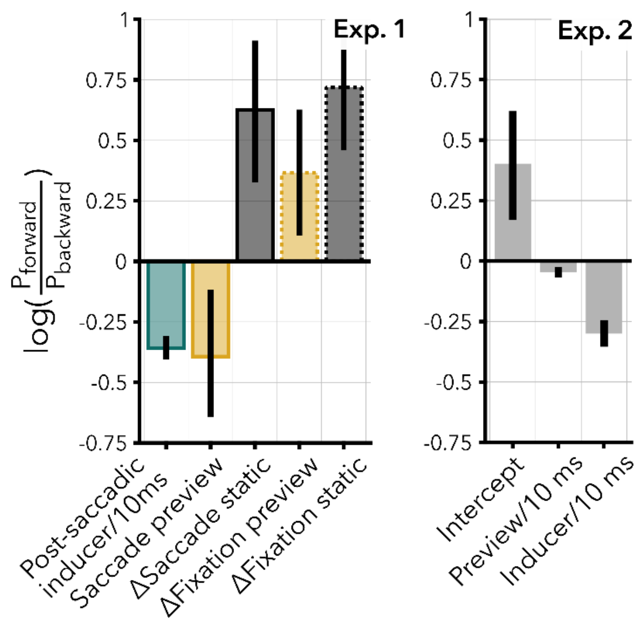

Figure 3. Bootstrapped coefficient estimates of the mixed effects model from Experiment 1 (left panel) and Experiment 2 (right panel). Estimates are obtained with non-parametric bootstrapping (2000 samples). Error bars represent empirical 95%-confidence intervals of the coefficient estimates. Experiment 1: the coefficient estimates of 'Saccade static', 'Fixation preview' and 'Fixation static' are

relative to the 'Saccade preview' condition. Experiment 2: the intercept refers to trials with 10 ms of preview and 10 ms of inducer.

Discussion

We examined spatiotopic updating of visual information across saccades. The current experiments demonstrate a fast updating mechanism in the visual system that predictively influences perception after an eye movement. We observed a direct link between post-saccadic perception and the strength of the pre-saccadic stimulus for stimuli that covered the parafovea after a saccade – in a control experiment (*SI Appendix*) we also observed this link for larger stimuli (inner, outer radius = [6.0, 9.25]°), in the same eccentricity range typically used in spatiotopic updating experiments (~5 to 10 degrees in the periphery). The time-scale on which this link is established is compatible with typical fixation durations observed in natural viewing (3) and represents a behavioral index of spatiotopic updating expressed as a perceptual bias in the direction of the pre-saccadic visual information, comparable to a 17.5 ms 'head start' in visual processing.

The current study differs in two important aspects from the studies with tilt-adaptation to assess the time-course of spatiotopic updating (37–39). First, the stimulus we used to assess spatiotopic updating is fast in nature. High phi can be induced in the order of tens of milliseconds, whereas tilt adaptation is typically induced in the order of hundreds of milliseconds (45). Second, the stimulus feature that had to be updated (inducer rotation direction) was stable and continuous across saccades, enabling the assessment of perceived visual continuity in an environment where the assumption of continuity across saccades is true (12, 46).

Rapid spatiotopic updating is plausible when considering the speed of processing in the human visual system, which contains stimulus specific representations rapidly after stimulus onset – in the order of 100 ms – as demonstrated in psychophysical studies (5, 6) and neuroimaging studies (4). This rapidly acquired information is used by the visual system to predict the sensory changes induced by saccades. It facilitates post-saccadic visual processing by anticipating the post-saccadic retinal input based on pre-saccadic input (49). Three fMRI studies support this idea by showing spatiotopic and feature-specific repetition suppression (50–52). Repetition suppression in neurophysiological measures is observed when the same stimulus is presented twice (53). Hence, repetition suppression in spatiotopic coordinates can be interpreted as a neurophysiological measure of the visual system regarding the post-saccadic stimulus to be 'the same' as the pre-saccadic stimulus, even though it was presented at different retinotopic coordinates. Although these effects are in line with the current findings, the time-scale of fMRI studies is limited by the slow BOLD response. Interestingly, a recent EEG study provides more direct neurophysiological correlate of our behavioral findings (54). Edwards and colleagues used time-resolved decoding of a post-saccadic stimulus while varying the correspondence between the pre- and post-saccadic stimuli. The post-saccadic stimulus could be decoded faster when it matched the pre-saccadic stimulus than when it was different from the pre-saccadic stimulus. This indicates that information about the pre-saccadic stimulus affects the neural responses to the post-saccadic stimulus in a way that suggests more efficient processing when the two stimuli match. The current results show that this fast facilitation in post-saccadic visual processing is not only reflected in neurophysiological measures but can be quantified in human behavior.

Still, although we observed spatiotopic updating on a short time-scale, we would not generalize the results to all stimuli in the visual field. The reason for this caution is that while there is ample evidence in favor of spatiotopic updating of visual information, there are also studies that fail to observe this with either behavioral measures (42, 55, 56) or with fMRI (57). One important restriction on spatiotopic updating seems to be that it is limited to attended stimuli, passive visual stimulation does not automatically result in spatiotopic updating (47, 58). The introspective feeling of visual continuity thus could arise from a match between the predicted post-saccadic retinal image and observed retinal image of an attended stimulus (49, 59).

Predicting upcoming stimuli is a fundamental characteristic of the brain, as stated by theories of predictive coding (60). Anticipating the consequences of an upcoming saccade is a frequently recurring example of a scenario where the principles of predictive coding are applied (61–63). This anticipation could be implemented as a forward model (64), where a corollary discharge from the oculomotor system enables the dissociation between internal and external changes in retinal input (65). Here, we observed effects of a spatiotopic prediction on post-saccadic perception within the temporal regime of the typical latencies of visually guided saccades. With these findings, rapid spatiotopic updating of visual information is a plausible mechanism that contributes to perceptual continuity across saccades in natural viewing.

Methods

Subjects

52 subjects (age: M = 22.6, range = [18,37], 26 female) with normal or corrected-to-normal acuity participated after giving written informed consent (N = 20 in Experiment 1, N = 12 in Experiment 2, N = 20 in *SI Appendix, Control Experiment*). The sample size of Experiment 1 was based on the effect sizes of our previous study with high phi (20). The sample size in Experiment 2 was lower because we planned to make fewer statistical comparisons with fewer experimental conditions. This study was approved by the local ethical committee of the Faculty of Social Sciences of Utrecht University. All subjects were naïve to high phi prior to the experiments and completed a screening procedure (*SI Appendix, screening*) to ensure they could reliably report the motion direction of a rotating annulus. Moreover, we verified whether subjects perceived backward steps with high phi after a long inducer (500 ms; *SI Appendix, screening;*

Fig. S2). One subject was excluded from the dataset of Experiment 1 because of a failure to meet this criterion (*SI Appendix, preprocessing*)

Setup

Stimuli were displayed on a 48.9º by 27.5º Asus RoG Swift PG278Q, an LCD-TN monitor with a spatial resolution of 52 pixels/º and a temporal resolution of 100 Hz (AsusTek Computer Inc., Taipei, TW). The ultra low motion blur backlight strobing option of the monitor was enabled (maximum pulse width) for higher temporal precision (66). Eye position of the left eye was recorded with an Eyelink 1000 at 1000 Hz (Sr Research Ltd., Mississauga, ON, Canada). The eye-tracker was calibrated using a 9-point calibration procedure. All stimuli were created and presented in Matlab 2016a (The Math Works, Inc., Natick, MA.) with the Psychophysics Toolbox 3.0 (67) and the Eyelink Toolbox (68). Visual onsets and eye-movement data were synchronized using photodiode measurements (*SI Appendix, synchronization*).

Stimuli

Stimuli were annuli (inner radius ≈ 3º, outer radius ≈ 6º) with random grayscale textures, created by low pass filtering random black (0.09 cd/m^2) and white (88.0 cd/m^2) pixels with a pillbox average (radius = 1.24º). For rotating annuli the rotational velocity was 20º/sec. Fixation targets were black dots (radius ≈ 0.2º) with a gray point in the center (radius ≈ 0.075º). All stimuli were presented on a uniform gray background (44.1 cd/m^2). We tested the spatial generalizability of the preview effect observed in Experiment 1 by repeating the saccade conditions using stimuli with different radii (*SI Appendix*).

Analysis

Before the statistical analysis, eye movement data were preprocessed (*SI Appendix, preprocessing*) and visual onsets were aligned to the eye movement data based on photodiode measurements (*SI Appendix, synchronization;* Fig S5). We analyzed the perceived step direction (i.e. the probability of a ‘forward step’ response: $p_{forward}$) with a logistic linear mixed effects model (69). $p_{forward} = \frac{2}{1+ e^{-(X\beta+Zy)}} - 1$, where X is the design matrix, β is a vector with the fixed effects coefficients, Z the random effects design matrix and y the random effect coefficients. All estimates of fixed effects coefficients are reported relative to the intercept condition, here the *Saccade preview* condition with an inducer of 10 ms (Fig. 1D). In Experiment 1, the mixed effects model contained fixed effects of inducer duration and condition, and random effects of inducer duration, condition and inducer rotation direction per subject (*SI Appendix, statistics Exp. 1*). Condition was modelled as a categorical variable and inducer duration as a continuous variable. We only allowed inducer durations between 10 and 60 ms. We did not include the interaction between condition and inducer duration because a model comparison showed that, all other things kept equal, the interaction did not improve the model ($\chi^2(3) = 4.16$, $p = 0.245$). We compared conditions among each other with planned contrasts. Reported p-values for planned contrasts are corrected with the Holm-Bonferroni method (70). In Experiment 2, the model contained fixed effects for pre-saccadic inducer duration and post-saccadic inducer duration, and random effects of pre-saccadic inducer duration, post-saccadic inducer duration and rotation direction per subject (*SI Appendix, statistics Exp. 2*). Both inducer durations were modelled as continuous variables. We used non-parametric bootstrapping to obtain 95%-confidence intervals of the estimated fixed effects coefficients. 2000 bootstrap samples were constructed by stratified sampling from the original dataset, with stratification according to the fixed effects but not the random effects. Trials were sampled with replacement. Bootstrapped coefficient estimates and 95%-confidence intervals are displayed in Fig. 3. Individual variation across these estimates are displayed in Fig. S3.

Saccade latencies

We set out to investigate spatiotopic updating across saccades unconstrained latencies. Saccade latencies in natural viewing conditions are typically around 250 ms (3). In Experiment 1, the average median saccade latency was 146 ms (range = 111-177 ms across subjects). In Experiment 2, the average median saccade latency was 136.8 ms (range = 112-178 ms across subjects).

Data availability

All scripts and data are publicly available at Open Science Framework: DOI 10.17605/OSF.IO/HX5WP

Acknowledgements

We thank Pieter Schiphorst for his assistance in the synchronization of eye-movement data with the timing of visual onsets. This work was supported by VIDI grant 452-13- 008 from the Netherlands Organization for Scientific Research to S.v.d.S.

References

1. Findlay JM, Gilchrist ID (2003) *Active Vision* (Oxford University Press, Oxford, UK) doi:10.1093/acprof:oso/9780198524793.001.0001.
2. Curcio CA, Sloan KR, Kalina RE, Hendrickson AE (1990) Human photoreceptor topography. *The Journal of Comparative Neurology* 292(4):497–523.
3. Henderson JM, Hollingworth A (1998) Eye movements during scene viewing: An overview. *Eye Guidance in Reading and Scene Perception*, ed Underwood G (Elsevier Science Ltd., Oxford), pp 269–293. 1st Ed.
4. Carlson T, Tovar DA, Alink A, Kriegeskorte N (2013) Representational dynamics of object vision: The first 1000 ms. *Journal of Vision* 13(10):1–1.
5. Kirchner H, Thorpe SJ (2006) Ultra-rapid object detection with saccadic eye movements: Visual processing speed revisited. *Vision Research* 46(11):1762–1776.
6. Crouzet SM (2010) Fast saccades toward faces: Face detection in just 100 ms. *Journal of Vision* 10(4):1–17.
7. Wandell BA, Dumoulin SO, Brewer AA (2007) Visual Field Maps in Human Cortex. *Neuron* 56(2):366–383.
8. Guthrie B, Porter J, Sparks D (1983) Corollary discharge provides accurate eye position information to the oculomotor system. *Science* 221(4616):1193–1195.
9. Sommer MA, Wurtz RH (2008) Visual Perception and Corollary Discharge. *Perception* 37(3):408–418.
10. Duhamel, Colby C, Goldberg ME (1992) The updating of the representation of visual space in parietal cortex by intended eye movements. *Science* 255(5040):90–92.
11. Walker MF, Fitzgibbon EJ, Goldberg ME (1995) Neurons in the monkey superior colliculus predict the visual result of impending saccadic eye movements. *Journal of Neurophysiology* 73(5):1988–2003.

12. Mirpour K, Bisley JW (2012) Anticipatory Remapping of Attentional Priority across the Entire Visual Field. *Journal of Neuroscience* 32(46):16449–16457.
13. Zirnsak M, Steinmetz NA, Noudoost B, Xu KZ, Moore T (2014) Visual space is compressed in prefrontal cortex before eye movements. *Nature* 507(7493):504–507.
14. Neupane S, Guitton D, Pack CC (2016) Two distinct types of remapping in primate cortical area V4. *Nature Communications* 7:10402.
15. Wang X, et al. (2016) Perisaccadic Receptive Field Expansion in the Lateral Intraparietal Area. *Neuron* 90(2):400–409.
16. Crapse TB, Sommer MA (2012) Frontal Eye Field Neurons Assess Visual Stability Across Saccades. *Journal of Neuroscience* 32(8):2835–2845.
17. Cicchini GM, Binda P, Burr DC, Morrone MC (2013) Transient spatiotopic integration across saccadic eye movements mediates visual stability. *Journal of Neurophysiology* 109(4):1117–1125.
18. Melcher D, Colby CL (2008) Trans-saccadic perception. *Trends in Cognitive Sciences* 12(12):466–473.
19. Higgins E, Rayner K (2015) Transsaccadic processing: stability, integration, and the potential role of remapping. *Attention, Perception, & Psychophysics* 77(1):3–27.
20. Fabius JH, Fracasso A, Van der Stigchel S (2016) Spatiotopic updating facilitates perception immediately after saccades. *Scientific Reports* 6(April):34488.
21. Jüttner M, Röhler R (1993) Lateral information transfer across saccadic eye movements. *Perception & Psychophysics* 53(2):210–220.
22. Wittenberg M, Bremmer F, Wachtler T (2008) Perceptual evidence for saccadic updating of color stimuli. *Journal of Vision* 8(14):1–9.
23. Demeyer M, De Graef P, Wagemans J, Verfaillie K (2009) Transsaccadic identification of highly similar artificial shapes. *Journal of Vision* 9(4):1–14.

24. Ong WS, Hooshvar N, Zhang M, Bisley JW (2009) Psychophysical Evidence for Spatiotopic Processing in Area MT in a Short-Term Memory for Motion Task. *Journal of Neurophysiology* 102(4):2435–2440.

25. Fracasso A, Caramazza A, Melcher D (2010) Continuous perception of motion and shape across saccadic eye movements. *Journal of Vision* 10(13):1–17.

26. Szinte M, Cavanagh P (2011) Spatiotopic apparent motion reveals local variations in space constancy. *Journal of Vision* 11(2):1–20.

27. Melcher D, Fracasso A (2012) Remapping of the line motion illusion across eye movements. *Experimental Brain Research* 218(4):503–514.

28. Harrison WJ, Bex PJ (2014) Integrating Retinotopic Features in Spatiotopic Coordinates. *Journal of Neuroscience* 34(21):7351–7360.

29. Oostwoud Wijdenes L, Marshall L, Bays PM (2015) Evidence for Optimal Integration of Visual Feature Representations across Saccades. *Journal of Neuroscience* 35(28):10146–10153.

30. Wolf C, Schütz AC (2015) Trans-saccadic integration of peripheral and foveal feature information is close to optimal. *Journal of Vision* 15(16):1–18.

31. Ganmor E, Landy MS, Simoncelli EP (2015) Near-optimal integration of orientation information across saccades. *Journal of Vision* 15(16):1–12.

32. Wolfe BA, Whitney D (2015) Saccadic remapping of object-selective information. *Attention, Perception, & Psychophysics* 77(7):2260–2269.

33. Zimmermann E, Weidner R, Fink GR (2017) Spatiotopic updating of visual feature information. *Journal of Vision* 17(12):1–9.

34. Jüttner M (1997) Effects of perceptual context on transsaccadic visual matching. *Perception and Psychophysics* 59(5):762–773.

35. Deubel H, Schneider WX, Bridgeman B (1996) Postsaccadic target blanking prevents saccadic suppression of image displacement. *Vision Research* 36(7):985–996.

36. Deubel H, Bridgeman B, Schneider WX (1998) Immediate post-saccadic information mediates space constancy. *Vision Research* 38(20):3147–3159.
37. Zimmermann E, Morrone MC, Fink GR, Burr D (2013) Spatiotopic neural representations develop slowly across saccades. *Current Biology* 23(5):193–194.
38. Nakashima Y, Sugita Y (2017) The reference frame of the tilt aftereffect measured by differential Pavlovian conditioning. *Scientific Reports* 7(June 2016):40525.
39. Zimmermann E, Morrone MC, Burr DC (2014) Buildup of spatial information over time and across eye-movements. *Behavioural Brain Research* 275:281–287.
40. Zimmermann E, Morrone MC, Burr DC (2013) Spatial Position Information Accumulates Steadily over Time. *Journal of Neuroscience* 33(47):18396–18401.
41. Zimmermann E, Morrone MC, Burr D (2015) Visual mislocalization during saccade sequences. *Experimental Brain Research* 233(2):577–585.
42. Knapen T, Rolfs M, Wexler M, Cavanagh P (2010) The reference frame of the tilt aftereffect. *Journal of Vision* 10(1):1–13.
43. Mathôt S, Theeuwes J (2013) A reinvestigation of the reference frame of the tilt-adaptation aftereffect. *Scientific Reports* 3(1). doi:10.1038/srep01152.
44. Gibson JJ, Radner M (1937) Adaptation, after-effect and contrast in the perception of tilted lines. I. Quantitative studies. *Journal of Experimental Psychology* 20(5):453–467.
45. Greenlee MW, Magnussen S (1987) Saturation of the tilt aftereffect. *Vision Research* 27(6):1041–1043.
46. Rao HM, Abzug ZM, Sommer MA (2016) Visual continuity across saccades is influenced by expectations. *Journal of Vision* 16:1–18.
47. Mirpour K, Bisley JW (2015) Remapping, spatial stability, and temporal continuity: From the pre-saccadic to postsaccadic representation of visual space in LIP. *Cerebral Cortex*:bhv153.

48. Wexler M, Glennerster A, Cavanagh P, Ito H, Seno T (2013) Default perception of high-speed motion. *Proceedings of the National Academy of Sciences of the United States of America* 110(17):7080–7085.

49. Herwig A (2015) Transsaccadic integration and perceptual continuity. *Journal of Vision* 15:1–6.

50. Dunkley BT, Baltaretu B, Crawford JD (2016) Trans-saccadic interactions in human parietal and occipital cortex during the retention and comparison of object orientation. *Cortex* 82:263–276.

51. Zimmermann E, Weidner R, Abdollahi RO, Fink GR (2016) Spatiotopic Adaptation in Visual Areas. *Journal of Neuroscience* 36(37):9526–9534.

52. Fairhall SL, Schwarzbach J, Lingnau A, Van Koningsbruggen MG, Melcher D (2017) Spatiotopic updating across saccades revealed by spatially-specific fMRI adaptation. *NeuroImage* 147(November 2016):339–345.

53. Grill-Spector K, Henson R, Martin A (2006) Repetition and the brain: Neural models of stimulus-specific effects. *Trends in Cognitive Sciences* 10(1):14–23.

54. Edwards G, VanRullen R, Cavanagh P (2018) Decoding trans-saccadic memory. *The Journal of Neuroscience* 38(5):0854–17.

55. Knapen T, Rolfs M, Cavanagh P (2009) The reference frame of the motion aftereffect is retinotopic. *Journal of Vision* 9(5):16.1–7.

56. Mathôt S, Theeuwes J (2013) A reinvestigation of the reference frame of the tilt-adaptation aftereffect. *Scientific Reports* 3:1152.

57. Lescroart MD, Kanwisher N, Golomb JD (2016) No evidence for automatic remapping of stimulus features or location found with fMRI. *Frontiers in Systems Neuroscience* 10(June):1–19.

58. Melcher D (2009) Selective attention and the active remapping of object features in trans-saccadic perception. *Vision Research* 49(10):1249–1255.

59. Cavanagh P, Hunt AR, Afraz A, Rolfs M (2010) Visual stability based on remapping of attention pointers. *Trends in Cognitive sciences* 14(4):147–53.

60. Rao RPN, Ballard DH (1999) Predictive coding in the visual cortex: A functional interpretation of some extra-classical receptive-field effects. *Nature* 2(1):79–87.

61. Friston K, Adams RA, Perrinet L, Breakspear M (2012) Perceptions as hypotheses: saccades as experiments. *Frontiers in Psychology* 3(May):1–20.

62. Spratling MW (2017) A predictive coding model of gaze shifts and the underlying neurophysiology. *Visual Cognition* 6285:1–32.

63. Vetter P, Edwards G, Muckli L (2012) Transfer of predictive signals across saccades. *Frontiers in Psychology* 3(JUN):1–10.

64. Crapse TB, Sommer MA (2008) The frontal eye field as a prediction map. *Progress in Brain Research* 171(08):383–390.

65. Cavanaugh J, Berman RA, Joiner WM, Wurtz RH (2016) Saccadic corollary discharge underlies stable visual perception. *Journal of Neuroscience* 36(1):31–42.

66. Zhang GL, et al. (2018) A consumer-grade LCD monitor for precise visual stimulation. *Behavior Research Methods*:1–7.

67. Kleiner M, Brainard DH, Pelli DG (2007) What's new in Psychtoolbox-3. *Perception* 36(14):1–16.

68. Cornelissen FW, Peters EM, Palmer J (2002) The Eyelink Toolbox: Eye tracking with MATLAB and the Psychophysics Toolbox. *Behavior Research Methods, Instruments, & Computers* 34(4):613–617.

69. Bates D, Mächler M, Bolker BM, Walker SC (2015) Fitting linear mixed-effects models using lme4. *Journal of Statistical Software*.

70. Holm S (1979) A simple sequentially rejective multiple test procedure. *Scandinavian Journal of Statistics* 6(2):65–70.

Supplementary Information for

The time course of spatiotopic updating across saccades

Jasper H. Fabius, Alessio Fracasso, Tanja C.W. Nijboer & Stefan Van der Stigchel

Correspondence should be addressed to: Jasper Fabius

Email: j.h.fabius@uu.nl

This PDF file includes:

Experimental Procedures

Experiment 1

With Experiment 1 we tested the hypothesis that visual information can be spatiotopically updated in a time window as short as the saccade latency. Subjects performed a gaze-contingent version of the high phi illusion (Fig. 1D). Each trial started with a drift check of 500 ms at the central fixation target (target radius ≈ 0.2º, radius of ROI for fixation control = 3º), followed by an additional fixation period of 250-500 ms. Then, an annulus with a random texture appeared, with its center 15º either to the left or to the right of the fixation target (equal probability). Subjects made a saccade to the center of the annulus. To increase the variability of the saccade latencies, we varied the synchrony of stimulus onset and fixation target offset with gaps of -150, 0 or 150 ms, taking advantage of the gap-effect (1). Saccades were slower with longer temporal overlap (Fig. S4). Importantly, before the saccade was executed, the annulus was either static *(Saccade static)* or rotated with 20º/s *(Saccade preview)*. In case of the *Saccade static* condition, the annulus started rotating during the saccade, i.e. as soon as gaze position was ≥3º away from the initial fixation target. The annulus rotated for another 20 or 50 ms after saccade offset (the post-saccadic inducer), i.e. when gaze was detected within ≤2º of the saccade target. Then, the texture of the annulus was rapidly replaced by four different random textures (20 ms/texture). Subjects indicated whether they perceived a rotational step clockwise or counterclockwise (2AFC). Responses were recoded to forward (1) and backward (-1) with respect to the rotation direction of the preceding inducer. Trials were presented in 12 blocks of 48 trials, where the following factors were presented factorially in random order within a block: preview (static/inducer), post-saccadic inducer duration (20/50 ms), inducer rotation direction (CW/CCW), saccade direction (L/R) and gap duration (-150/0/150 ms).

Subjects also performed two control conditions in separate blocks to test whether high phi can also be induced for a transient around fixation but with an inducer in the periphery. In these conditions we matched the visual input as close as possible to the saccade conditions while subjects maintained fixation during the whole trial (Fig. S1A). Subjects were presented a fixation target in the center of the screen. After 250-500 ms of stable fixation, an annulus with a random texture appeared in the periphery, at the same location as in the Saccade conditions. Again, this peripheral annulus was either static *(Fixation static)* or rotated with 20º/s *(Fixation preview)*. For each trial, the duration of the peripheral annulus was sampled from the distribution of saccade latencies that were collected in the saccade conditions. The distributions were estimated via non-parametric kernel density estimation, bounded on the closed interval [80, 500] ms. This sampling procedure was performed per individual subject, to match the durations of visual input between conditions with and without saccades as accurately as possible (Fig. S1B). Next, the peripheral stimulus disappeared, and the screen was blank (apart from the central fixation point) for a duration that was sampled from the smoothed distribution of saccade durations in the conditions with saccades. This sampling procedure was similar to the aforementioned sampling procedure, with the difference that it was bounded on the closed interval [20, 80] ms (Fig. S1C). The blank was followed by an annulus presented around the central fixation target. This annulus had the same random texture as the peripheral annulus and rotated for 20 or 50 ms (akin to the post-saccadic inducer in the conditions with a saccade). Then, the texture was replaced by four other random texture (20 ms/texture), after which subjects gave their response. In the *Fixation static* condition, we implemented an additional 'post-saccadic inducer' duration of 500 ms, to test whether a long, and therefore strong, inducer reliably induces the high phi illusion in every subject. We used the *Fixation preview* condition to test for a spatially invariant effect of the inducer. Blocks with and without saccades were interleaved. Before the start of the experiment, subjects practiced one block with and one without saccades. For the actual experiment subjects completed 6 blocks of the Fixation conditions and 12 blocks of the Saccade conditions.

Experiment 2

The data from Experiment 1 show that even within a time window as brief as the latency of a visually guided saccade, pre-saccadic perception of a stimulus biases post-saccadic perception of the same spatiotopically localized stimulus. With Experiment 2 we examined whether the duration of the pre-saccadic preview affects the strength of the post-saccadic bias. As suggested previously, spatiotopic updating might become detectable with behavioral measures only when sufficiently long saccade latencies are allowed. Here, we worked the other way around, where we tried to minimize the observed spatiotopically induced bias, since we already observed a bias with short saccade latencies. Therefore, we decoupled saccade latency and preview duration in Experiment 2 by making each preview a mixture of a static preview followed by an inducer preview. Yet note that under natural viewing conditions, the preview duration is as long as the saccade latency (like in Experiment 1). The task in Experiment 2 was similar to Experiment 1. However, rather than being presented with either a static preview or an inducer preview (Experiment 1), subjects were presented with a mixture of both (Fig. 2A). Specifically, when the annulus appeared in the periphery, it started rotating after a delay 0, 50, 100 or 150 ms. Again, subjects were instructed to make a saccade to the center of the annulus immediately after the onset of the annulus. Thus, the total inducer preview duration was determined both by the saccade latency of the subjects and the rotation delay of the stimulus and continued rotating for either 20 or 50 ms after saccade offset. Additionally, subjects performed trials where they maintained fixation, and the inducer and transient were presented around the fixation point. These trials included no peripheral inducers. Subjects practiced one block of the Saccade condition, and one block of the Fixation condition. In the actual experiment, subjects completed 6 blocks of 24 trials of the Fixation condition and 24 blocks of 32 trials of the Saccade condition.

Screening

Long inducers – The high phi illusion is a subjective, non-random interpretation of a random stimulus: the direction of the transiently changing textures is interpreted as a large rotational step in backwards direction with respect to the preceding rotational motion. To make sure the illusion could successfully be induced in all subjects, we verified the perceptual interpretation of the transient after a long inducer (500 ms) in the *Fixation static* conditions in both experiments. An inducer of 500 ms should evoke a strong percept of a large backward step (cf. Wexler et al. 2013; Fabius et al. 2016). Subjects would be excluded when their binomial confidence interval would include 0, i.e. no clear sign of a successfully induced high phi illusion with a strong inducer. All but 1 subject reliably reported backward jumps with this long inducer (Fig. S2). One subject was excluded from the analysis based on this criterion (Subject 19 in Experiment 1).

Large physical step – Because the high phi illusion is a subjective measure, we verified whether subjects were able to accurately dissociate the direction of a physical rotational step – i.e. not illusory – from the rotation direction of a slowly rotating inducer. All subjects performed a screening experiment prior to the main experiment. In the screening, subjects fixated a fixation target on the left (-10º), center (0º) or right (10º) side of the screen. A static annulus appeared after 500 ms of stable fixation at the fixation target (i.e. all recorded gaze samples were within 3º of the fixation target). The annulus remained static for 600 ms, and then rotated clockwise or counterclockwise for 1000 ms., akin to a long inducer in the high phi illusion. Rotational velocity was 20º/sec, i.e. rotational steps of 0.2º presented at 100 Hz (the refresh rate of our monitor). After the rotation, the annulus made a rotational step of 12º and stopped rotating. Subjects indicated the direction of the large step by pressing the left arrow (‘counterclockwise’) or right arrow (‘clockwise’). The direction of the large step, the direction of the preceding rotational motion and the location were counterbalanced over 36 trials (3 repetitions per combination). To assess accuracy, we computed the proportion correct responses over all trials. Every subject performed well above chance level ($p = 0.5$) in Experiment 1 ($M = 0.95$, range = 0.81-1.00) and Experiment 2 ($M = 0.97$, range = 0.75-1.00).

Control experiment

Introduction

To investigate spatiotopic updating for more peripheral targets we decided to test the preview effect from Experiment 1 with stimuli of different sizes. The rationale here is that although the annuli in Experiment 1 are not stimulating the fovea after the saccade – and so do not coincide with the saccade target – they are closer to the fovea (inner radius of the annulus = 3°) than typically seen in similar experiments on spatiotopic updating, which is usually between 5 and 10 degrees. In this control experiment, we used annuli with different radii than in Experiment 1, one smaller (inner radius = 2.6°, outer radius = 5°) and one larger (inner radius = 6°, outer radius = 9.25°). It is important to remark that the eccentricity range for the large annulus lies in the same eccentricity regimes typically seen in spatiotopic updating experiments (5-10 degrees in the periphery). Most importantly, the larger annulus' distance from the initial fixation point and the saccade target is almost the same on the vertical midline of the screen, i.e. the retinal stimulation before and after the saccade was parafoveally (2). See Figure C1 for an illustration of these sizes. When accounting for the cortical magnification factor, the surface of these two sizes was roughly equal, although smaller than the surface of the stimuli in Exp. 1 and Exp. 2.

Methods

We repeated the Saccade conditions from Experiment 1, i.e. 50% of trials contained a preview of the inducer before saccade onset, on the other 50% the inducer was static until the saccade had started. Additionally, the annulus could be large or small. Within a block of 64 trials, all unique combinations of preview (with/without), annulus size (small/large), saccade direction (left/right), rotation direction (cw/ccw) and inducer duration (20/50 ms) were repeated twice. Subjects completed 15 of these blocks.

Additionally, before the Saccade conditions, subjects completed 3 blocks of a Fixation condition, where subjects were required to maintain fixation at a fixation point (either on the left or right side of the screen, similar to the locations used in the Saccade conditions). The High phi illusion was then presented around that fixation point. Each block in the Fixation condition consisted of 48 trials.

Similar to Exp. 1 and Exp. 2, we only included participants who scored above chance level on a screening test, where we presented an inducer of 1 s, followed by a physical step of 12°. Next, we only included data in the analysis from participants who reliably reported backward jumps after a long inducer (500 ms) in an additional Fixation condition. 2/20 subjects were excluded based on the second criterion. Additionally, we applied the same inclusion criteria that are summarized in the *SI Appendix* (*Preprocessing*). In Exp. 3, the 95^{th} percentile of saccade latencies (inclusion criterion 6) was 480 ms, and the 2.5^{th} and 97.5^{th} percentiles of the manual response times were 310 and 1413 ms.

Analysis of the data was identical to the analysis of Experiment 1. We analyzed the data for the small and large stimuli separately with generalized linear mixed effects models. These models had the same fixed and random effects structure as the model that was used to analyze Exp. 1. With these models, we performed non-parametric bootstrapping to obtain 95% confidence interval of the fixed effect coefficients and model predictions.

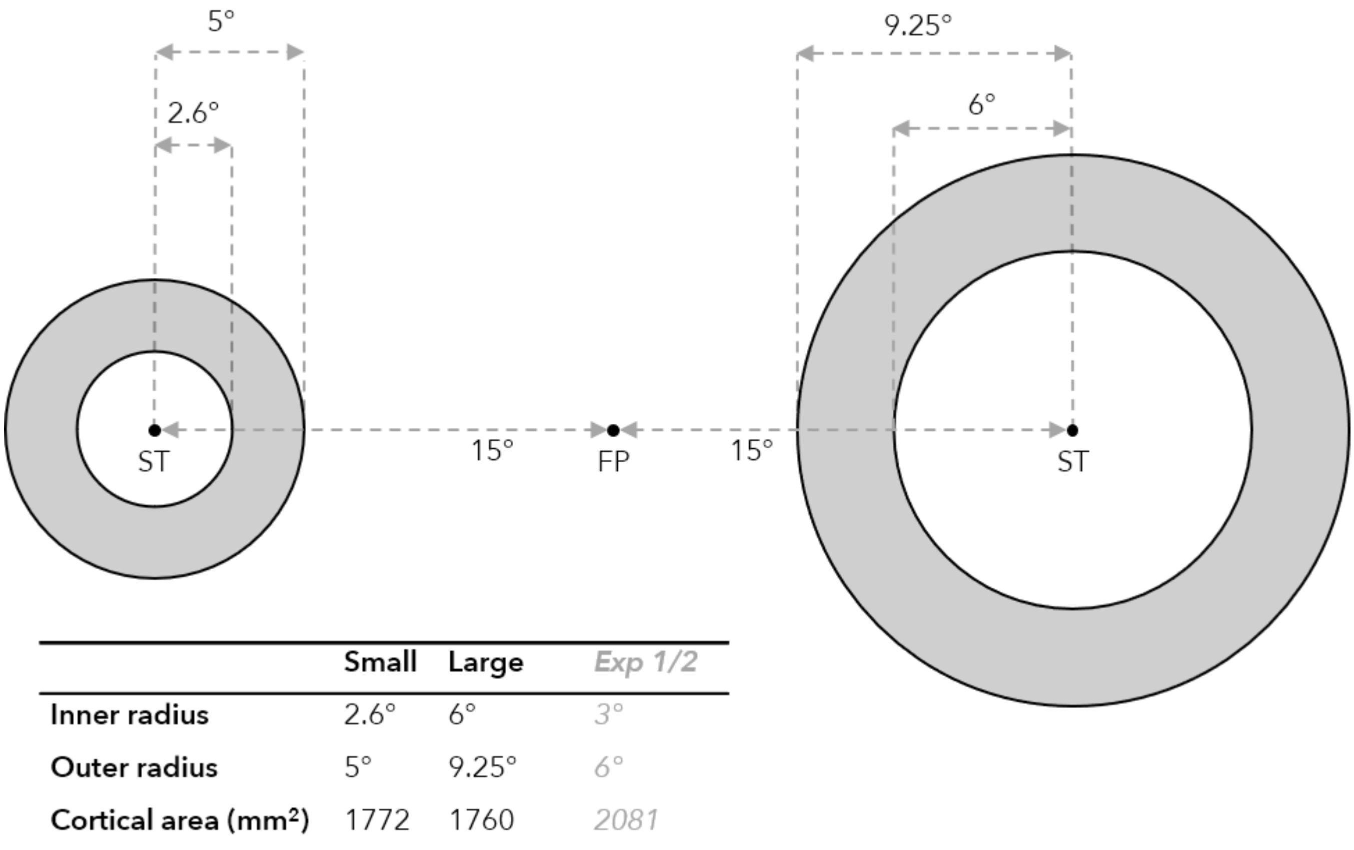

	Small	Large	Exp 1/2
Inner radius	2.6°	6°	*3°*
Outer radius	5°	9.25°	*6°*
Cortical area (mm²)	1772	1760	*2081*

Figure C1. *Design of the control experiment. The size of the stimulus was changed with respect to Experiment 1 and 2. One annulus had a slightly smaller inner and outer radius than the annulus used in Experiments 1 and 2, and the other annulus had an inner radius that was similar to the outer radius as the annulus in Experiment 1 and 2. The surface of these two annuli were roughly comparable when accounting for the cortical magnification factor, although smaller than the stimuli used in Experiment 1 and 2. FP = initial fixation point. ST = saccade target, only one saccade target and stimulus would be shown on each trial. Stimulus sizes were counterbalanced across screen sides.*

Results

The average median saccade latencies in trials with the small annulus was 161 ms (range = 117-261 ms), and 164 ms in trials with the large annulus (range = 119-276 ms).

Both for the small and the large annulus, the perceived step direction became more biased to backward steps with increased post-saccadic inducer durations (small annulus: $\beta = -0.23$, 95%-CI = [-0.29, -0.16], $F(1, 4953) = 90.58$, $p < 0.001$; large annulus: $\beta = -0.42$, 95%-CI = [-0.51, -0.31], $F(1, 3640) = 88.15$, $p < 0.001$). So, for both annulus sizes, the High phi illusion could reliably be induced.

Regarding the preview effect for the small annulus, the observed bias in the Saccade Static condition was smaller than in the Saccade Preview condition ($\Delta\beta = 0.48$, 95%-CI = [0.29, 0.69], $F(1, 4953) = 5.48$, $p = 0.019$). Similarly, for the large annulus the observed bias in the Saccade Static condition was also smaller than in the Saccade Preview condition ($\Delta\beta = 0.60$, 95%-CI = [0.25, 0.93], $F(1, 3640) = 7.20$, p

= 0.007). To estimate the size of the preview benefit in time we took the ratio between the effect of the post-saccadic inducer per 10 ms and the difference between the Saccade static and Saccade preview conditions. For the small annulus this preview benefit is 20.9 ms (bootstrapped 95%-CI = [11.6, 32.2] ms), for the large annulus this is 14.3 ms (bootstrapped 95%-CI = [7.4, 24.6] ms). See Figure C2 for an illustration of the estimated perceived step direction per condition and per inducer duration for the two different annulus sizes. See Figure C3 for the bootstrapped model estimates.

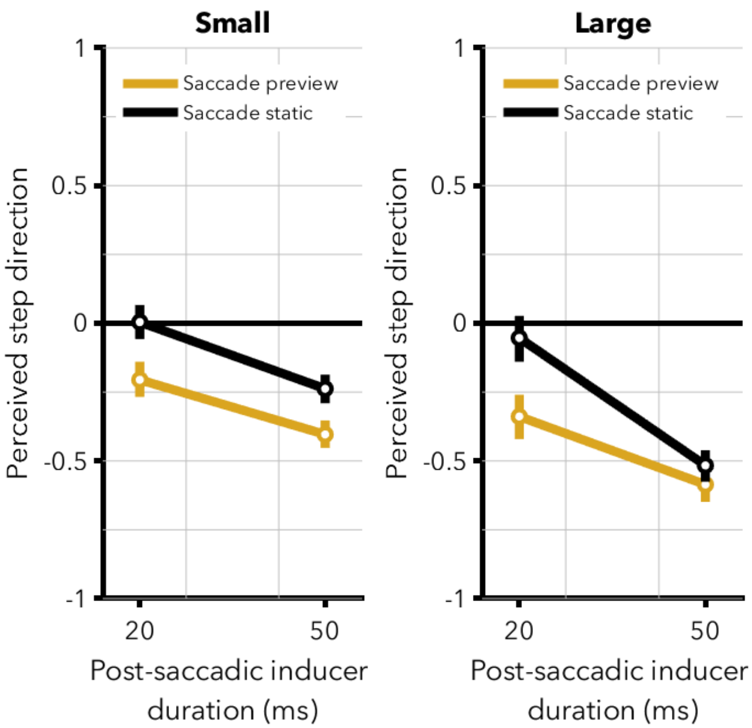

Figure C2. *Model estimates of the average perceived step direction, where the error bars represent the 95%-CI of the estimates obtained with non-parametric bootstrapping. The perceived step direction became more biased to backward steps with increased post-saccadic inducer duration both for the small and the large annulus. Additionally, there was a stronger bias in the Saccade preview condition (yellow) than in the Saccade static condition (black), for both annulus sizes.*

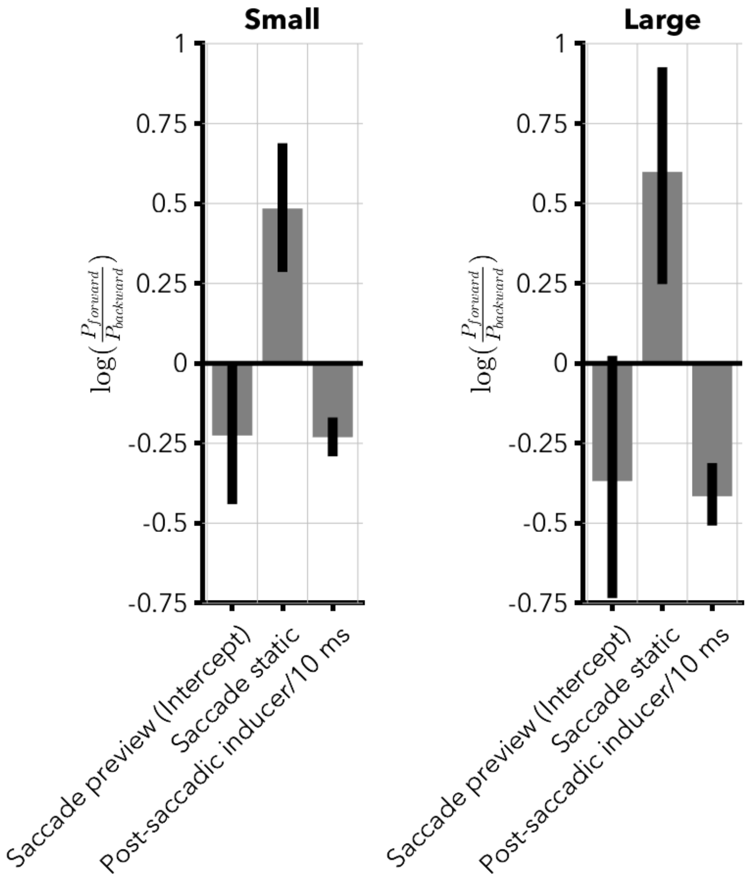

Figure C3. *Bootstrapped coefficient estimates of the generalized linear mixed effects model from trials with a small annulus (left panel) and trials with a large annulus (right panel). Estimates are obtained with non-parametric bootstrapping (2000 samples). Error bars represent empirical 95%-confidence intervals of the estimated coefficients. The estimated coefficients of the 'Saccade static' conditions are relative to the 'Saccade preview' conditions in each panel. The bias to backward steps is observed in the Saccade preview condition is larger than in the Saccade static for both the small and the large annulus.*

Discussion

In this control experiment, we replicated the spatiotopic preview effect from Experiment 1. Moreover, we measured and observed spatiotopic updating of the inducer effect for an annulus that was presented in the peripheral, parafoveal visual field. This larger annulus stimulated peripheral parts of the visual field in which previous effects of spatiotopic updating have also been observed. These findings demonstrate that rapid spatiotopic updating can be observed at different locations than the saccade target.

Data analysis

Preprocessing

We only included subjects who could reliably report the direction of rotational steps in the screening (Experiment 1: N = 20/20, Experiment 2: N = 12/12) and whose responses showed a successful induction of the high phi illusion in trials with a long inducer (500 ms) in the *Fixation static* condition (Experiment 1: N = 19/20, Exp. 2: N = 12/12). One subject (Experiment 1) was excluded because she did not report significantly more backward steps when the high phi illusion was presented with this long inducer (Fig. S2). Even though our paradigm was gaze-contingent, we determined post-saccadic inducer durations offline. Saccades were detected offline using the native SR Research saccade detection algorithm. The timing of the onset of the stimuli was determined by the timestamps in the Eyelink datafile, corrected for the input lag of 11 ms of the monitor, as measured with a photodiode (*SI appendix*, *Synchronization*). Next, we only included trials in the analysis where

1) the primary saccade had an amplitude > 12º
2) the primary saccade started and ended within 2º of the fixation points (or, in case of Fixation conditions, where the median gaze position over 50 ms after preview onset and inducer onset was within 2º of the fixation points)
3) the primary saccade started before the gaze-contingent onset (at least 10 ms)
4) the primary saccade ended after the gaze-contingent onset (at least 10 ms)
5) the primary saccade had a minimum latency of 80 ms after stimulus onset
6) the primary saccade had maximum latency no higher than the 95^{th} percentile of all saccades that were included after applying criteria 1 to 4 (Experiment 1: 320 ms, Experiment 2: 242 ms)
7) where the manual response time was within the 2.5^{th} and 97.5^{th} percentile of all the trials after applying criteria 1 to 4 (Experiment 1: 331-1244 ms, Experiment 2: 320-1240 ms)
8) where the post-saccadic inducer duration was in the closed interval [20, 60] ms in Exp. 1, or [10, 60] in Exp. 2.
9) Another inclusion criterion in Experiment 2 was that the inducer preview duration had to be in the closed interval [10, 140] ms.

With these criteria we included 7962 trials in Experiment 1 (42.9% of all trials) and 5436 trials in Experiment 2 (49.7% of all trials). For the main analysis of Experiment 2, only the trials from the saccade condition were used (3802 trials, 41.3% of all saccade trials).

Synchronization of visual onsets and eye-movements

Introduction – For the analysis of the reported experiments, we synchronized eye-movement data from the Eyelink data file (EDF) with stimulus onset (as determined by the timestamps in the EDF). During the experiments, timestamps were sent to the EDF immediately after PsychToolbox reported that the vertical retrace had started. That is, we used the function Eyelink('Message') immediately after using Screen('Flip'). With these timestamps in the EDF, we determined in which trials our online-gaze contingent algorithm performed correctly (e.g. starting the rotation of the inducer during the saccade rather than after the saccade in the *Saccade static* condition). Hence, to ensure that we only included trials where the stimulus was indeed rotating before the saccade had ended, we only included trials where the time difference between the timestamp of the onset of the inducer and the offset of the saccade was larger than 10 ms (i.e. the duration of 1 frame at 100 Hz). This criterion was also applied to Induce Preview trials. Thus, we entered only those trials in the analysis where the gaze-contingent onset was at least 10 ms before the offset of the saccade. This method of synchronizing stimulus presentation with eye movement data is only valid if the timestamp in the EDF was indeed synchronized with stimulus onset. However, this is most likely not the case for most LCD monitors because they suffer from input lag (a delay introduced in the hardware of the monitor). To accurately synchronize eye movement data and visual stimulation we measured the input lag of our monitor with a photodiode that was fed directly into the printer port of the Eyelink host PC.

Methods – We used a photodiode (sampling rate = 10 kHz) connected to an Itsy Bitsy microcontroller board (Adafruit Industries, New York City, NY). The output of the Itsy Bitsy was sent to the parallel port (printer port) of the Eyelink host PC, to the 11^{th} pin ('busy' pin). With a custom-written Matlab script, using the Psychophysics toolbox and Eyelink toolbox, we changed the luminance of the screen every frame. We tested 4 transition transitions from full dark to 25%, 50%, 75% or 100% luminance. Luminance thresholds for the output were set to 80% of the required luminance level in a given measurement. After the script commanded a luminance change (with the Psychophysics toolbox's Screen('Flip') function) a message was sent to the Eyelink data file (using the Eyelink toolbox's Eyelink('Message') function). Simultaneously, we recorded the output of the photodiode directly into the Eyelink data file. We should note that our LCD monitor uses a feature that is not common in all LCD monitors, called 'ultra low motion blur' (ULMB). With ULMB turned on, the backlight of the LCD panel is strobing at the same rate as the refresh rate of the monitor, in our case 100 Hz (see Fig. S5 for measurements made with oscilloscope). This makes the monitor effectively similarly suited for visual psychophysics as traditional CRT monitors, as recently described by Zhang and colleagues (2018). Because the backlight is strobing, this means that a transition from 100% bright to 50% bright is in fact a transition from 100% to 0% to 50% luminance. We made several photographs from measurements with an oscilloscope to demonstrate this feature of the screen (Figure S6). Given that the screen is always dark between two frames, and the photodiode is a binary signal, we can only consider changes from dark to a certain luminance value. For each luminance level, we reversed the luminance 2000 times (i.e. 1000 from bright to dark and 1000 from dark to bright). We compared the differences between the timestamp of the message and the time of change in photo diode output.

Results and discussion – There was a consistent delay of 11.0 ms (s.d. = 0.5 ms) between the timestamp and the time of contrast reversal as measured with the photodiode (Fig. S6A). This is numerically similar to the input lag measured by Zhang and colleagues (3). The delays were similar across different vertical locations. To correct for the measured input lag, we added 11 ms to all the timestamps in the EDF that indicated the onset of a visual stimulus before we performed our analyses and before we applied the in/exclusion criteria to individual trials. Timings of post-saccadic inducer onsets over eye-positions are visualized in Fig. S6B.

Statistics Experiment 1

We analyzed the responses from Experiment 1 with four factors in the following model, with a logit link function. The analysis was run in Matlab 2016a, with the 'fitglme' function from the Statistics package.

Model structure

Experiment 1 was designed to test for effects of post-saccadic inducer duration and differences in offset between conditions. Thus, we constructed a mixed model with two fixed effects, one for condition and one for post-saccadic inducer duration. For completeness, we compared the model with these fixed effects against two alternative models with different fixed effects (see below). For the random effects, we allowed the size of the fixed effects to vary across subjects, because in most psychophysical experiments the effect sizes can vary across observers. Additionally, we added a random effect of rotation direction that we allowed to vary per subject. This third random effect was included to dissociate a perceptual bias from a response bias. There is a two stage rationale for this. First, the number of trials per rotation direction could not be balanced a priori, because the trial exclusion based on saccade parameters was performed pos-hoc. Second, theoretically, subjects could have a default response of, for example, pressing the 'right' button. If a subject with such a bias would also have more trials – after trial exclusion – with counterclockwise rotations, it would seem as though this subject would have a perceptual bias for reporting backward steps, whereas in fact he was just pressing the same button and hence a response bias. We account for this possibility by adding a random effect of rotation direction to vary per subject.

Formula

```
response ~ condition + inducer + (1 + condition + inducer + rotation | subject)
```

Factors

	Factor	Class	Levels	Code
0	Response	Categorical	backward forward	0 1
1	Condition	Categorical	saccade preview fixation static fixation preview saccade control	0 1 2 3
2	Post-saccadic inducer duration	Continuous	20 ms ⋮ 60 ms	1 ⋮ 5
3	Inducer rotation direction	Categorical	clockwise counterclockwise	0 1
4	Subject	Categorical	1 ⋮ 19	1 ⋮ 19

Model comparison

The design of the model for the analysis of Experiment 1 was defined by our experimental questions. However, we did examine whether adding an interaction term to the model would improve the fit. In addition, as a sanity check we compared our model against a model with the same random effects, but without any fixed effects.

Final model

```
response ~ condition + inducer + (1 + condition + inducer + rotation | subject)
```

Interaction model

```
response ~ condition * inducer + (1 + condition + inducer + rotation | subject)
```

Null model

```
response ~ 1 + (1 + condition + inducer + rotation | subject)
```

Final model vs. Interaction model

Theoretical Likelihood Ratio Test

Model	DF	AIC	BIC	LogLik	LRStat	deltaDF	pValue
finalModel	*26*	*8775*	*8956.5*	*-4361.5*			
interactionModel	*29*	*8776.8*	*8979.3*	*-4359.4*	*4.155*	*3*	*0.2452*

Final model vs. Null model

Theoretical Likelihood Ratio Test

Model	DF	AIC	BIC	LogLik	LRStat	deltaDF	pValue
nullModel	*22*	*8795.5*	*8949.1*	*-4375.8*			
finalModel	*26*	*8775*	*8956.5*	*-4361.5*	*28.543*	*4*	*9.6774e-06*

Bootstrapped GLME estimated coefficients.

Coefficients obtained with non-parametric empirical bootstrapping. For the bootstrapping procedure we randomly sampled an equal number of responses per inducer duration per condition as in the original model (i.e. stratification over the fixed effects), without stratifying over the random effects (i.e. subject and rotation direction). Thus, for each sample we had 7962 observations, and we re-fitted our original model with these random sample of trials. This sampling and re-fitting was repeated 2000 times. To obtain confidence intervals on the estimated coefficients, we calculated empirical confidence intervals. That is, taking the difference between the original model estimates and all the bootstrap estimates: $\boldsymbol{\delta} = \mathbf{b}_{\mathbf{bootstrap}} - \mathbf{b}_{\mathbf{model}}$. The bias-corrected estimate of a given coefficient is defined as $\mathbf{b} = \mathbf{b}_{\mathbf{model}} - \boldsymbol{\delta}_{\mathbf{0.5}}$, and the 95% confidence interval is $[\mathbf{b}_{\mathbf{model}} - \boldsymbol{\delta}_{\mathbf{0.025}}, \mathbf{b}_{\mathbf{model}} - \boldsymbol{\delta}_{\mathbf{0.975}}]$.

Planned comparisons between conditions.

All estimated coefficients in the mixed effects model of Experiment 1 are relative to the *Fixation static* condition with a post-saccadic inducer of 20 ms. However, to answer all our experimental questions we also compared conditions among each other with planned comparisons. The reported p-values are Holm-Bonferroni corrected for multiple comparisons. Stars indicate a significant difference with an alpha of 0.05.

```
Saccade preview  vs Fixation static,  F(1, 7957) = 36.80, p < 0.0001*
Saccade preview  vs Fixation preview, F(1, 7957) = 10.13, p = 0.0059*
Saccade preview  vs Saccade static,   F(1, 7957) = 17.54, p = 0.0001*
Fixation static  vs Fixation preview, F(1, 7957) = 7.85,  p = 0.0153*
Fixation static  vs Saccade static,   F(1, 7957) = 0.90,  p > 0.05
Fixation preview vs Saccade static,   F(1, 7957) = 2.14,  p > 0.05
```

Statistics Experiment 2

Model comparison

Formulae

Final model

```
response ~ preview + inducer + (1 + preview + inducer + rotation | subject)
```

Interaction model

```
response ~ preview * inducer + (1 + preview + inducer + rotation | subject)
```

Null model

```
response ~ inducer + (1 + preview + inducer + rotation | subject)
```

Final model vs. Interaction model

Theoretical Likelihood Ratio Test

Model	DF	AIC	BIC	LogLik	LRStat	deltaDF	pValue
finalModel	*13*	*4041.0*	*4122.2*	*-2007.5*			
interactionModel	*14*	*4040.6*	*4128.0*	*-2006.3*	*2.3889*	*1*	*0.1222*

Final model vs. Null model

Theoretical Likelihood Ratio Test

Model	DF	AIC	BIC	LogLik	LRStat	deltaDF	pValue
nullModel	*12*	*4048.0*	*4122.9*	*-2012*			
finalModel	*13*	*4041.0*	*4122.2*	*-2007.5*	*8.9919*	*1*	*0.0027*

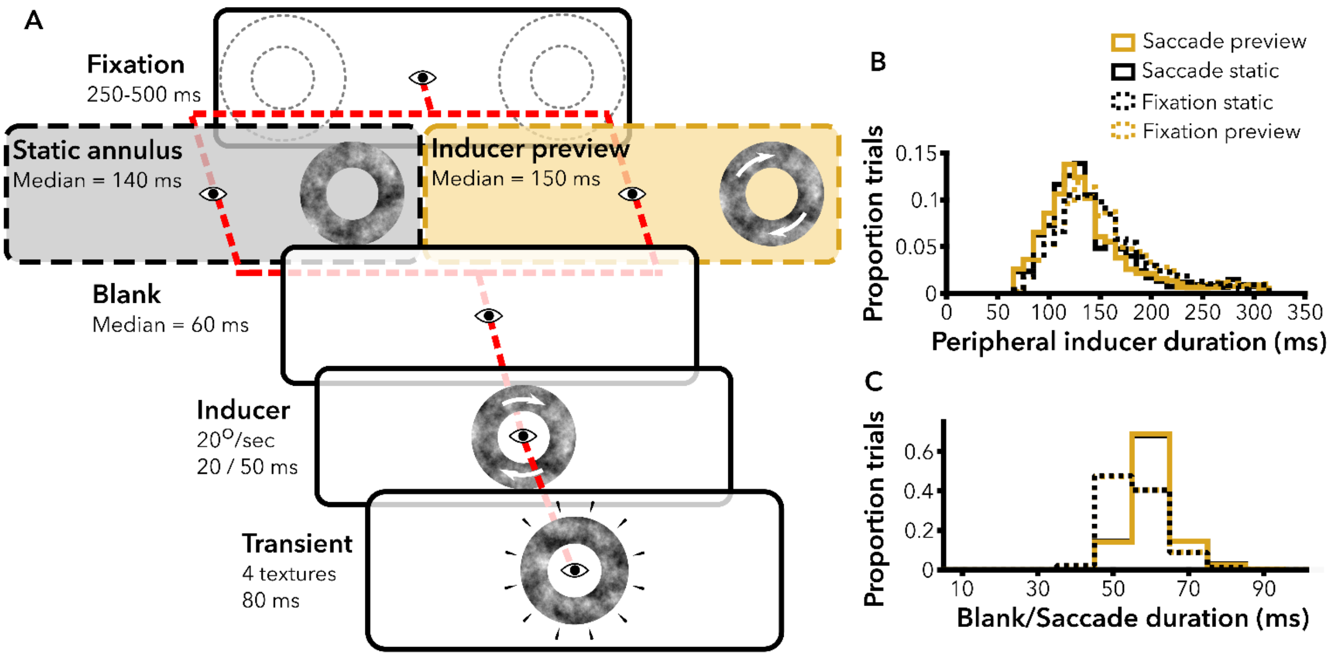

Fig. S1. A) Experiment 1, control conditions. The visual input from the experimental saccade conditions was mimicked as close as possible, without the execution of a saccade. The two control conditions proceeded almost identically, with the only exception that the peripheral annulus (panel 2) remained static (Fixation static) or rotated (Fixation preview). Subjects maintained fixation at a fixation target in the center of the screen over the entire course of a trial. The dotted lines in the first panel were not visible but merely illustrate the stimuli could appear at two locations (equal probability). The eye indicates required gaze position in each panel. Arrows on the annulus illustrates that the annulus rotated in that phase of the trial. Median duration of the peripheral stimulus (panel 2) and the blank (panel 3) were sampled from the saccade parameters from the experimental conditions. **B)** Histogram with durations of peripheral preview in control and experimental conditions from Experiment 1. The duration of the peripheral inducer in the control conditions (dashed lines) was sampled online from the distribution of saccade latencies (for each subject individually. Durations of the saccade latencies (solid lines) are corrected for the delay between timestamp and visual onset. **C)** Histogram with the durations of the blanks in the control conditions (dashed lines) and saccade durations (solid lines) in the experimental conditions. The duration of the blank in the control conditions was sampled from the distribution of the saccade durations in the experimental conditions.

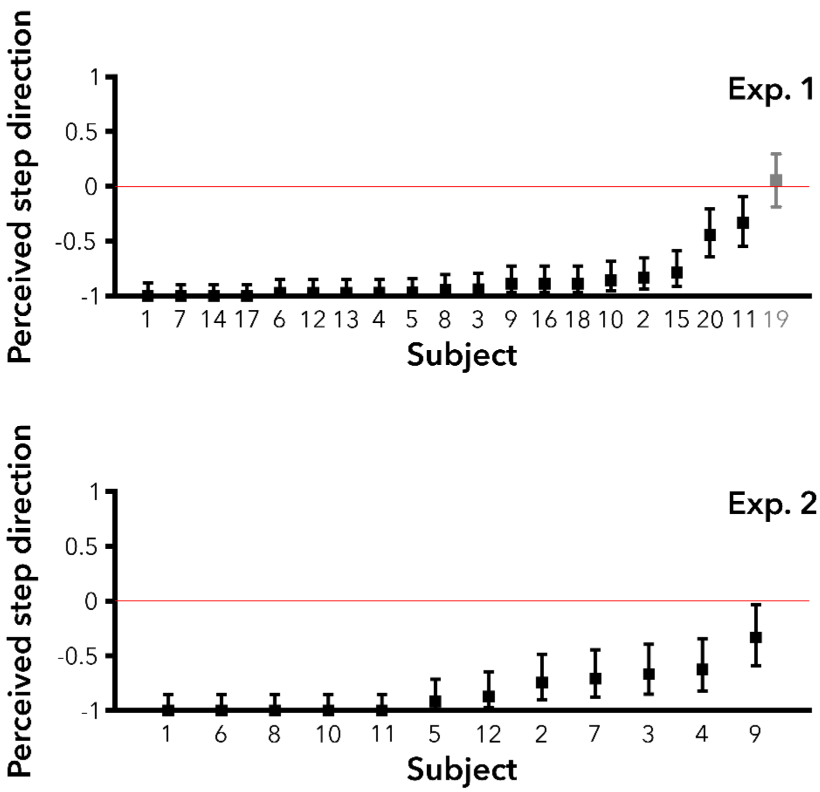

Fig. S2. Perceived step direction in the Fixation static condition with an inducer duration of 500 ms. Upper panel Experiment 1. Lower panel Experiment 2. Forward steps are coded +1 and backward steps -1. The average response for each subject is plotted. Subjects are ordered by the strength of their response bias. Error bars represent the binomial 95%-confidence interval.

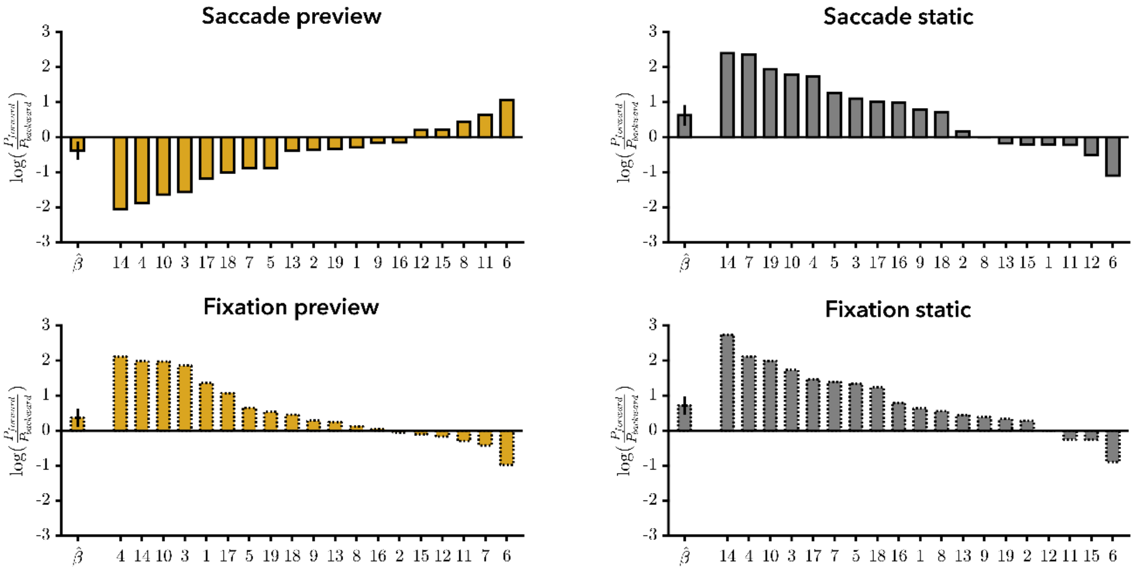

Fig. S3. Individual biases per condition in Experiment 1. First bar is the bias as estimated by the generalized linear mixed effects model (error bars are 95% bootstrapped confidence intervals). X tick labels refer to subject ID. In each panel, subjects are ordered by effect size. For each subject, the average response (converted to log odds) per condition with a post-saccadic inducer of 20 or 50 ms. The difference between these averages was divided by 3 to get an estimate of the effect of the post-saccadic inducer of 10. Then, we took the average response after 20 ms of post-saccadic inducer and subtracted the effect of 10 ms inducer. Thus, we had an estimate of the bias after 10 ms of post-saccadic inducer per condition per subject.

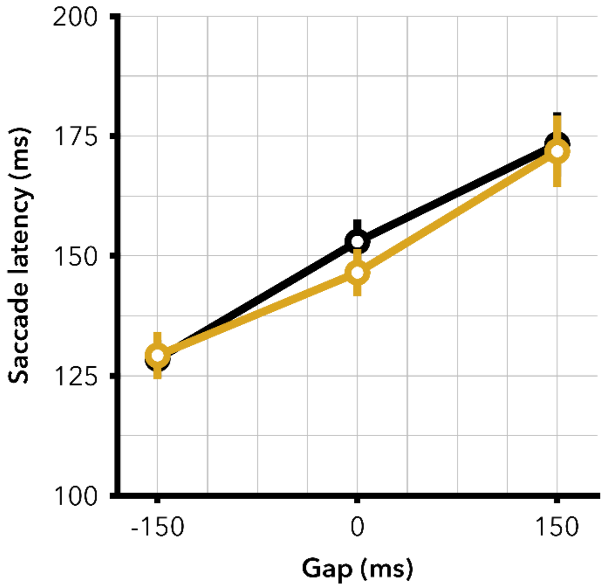

Fig. S4. Average saccade latencies in Experiment 1 in the Saccade Preview (yellow) and Saccade static (black) conditions. Error bars represent 1 standard error of the mean over subjects. Gap duration is defined as the time of fixation target offset minus the time of stimulus onset. A two-way repeated measures analysis of variance showed the gap modulation had a significant effect on saccade latencies ($F(2,36) = 31.815$, $p < 0.001$), with no significant difference between the two preview conditions ($F(1,18) = 1.065$, $p = 0.316$), nor a significant interaction between gap duration and preview condition ($F(2,36) = 1.298$, $p = 0.285$).

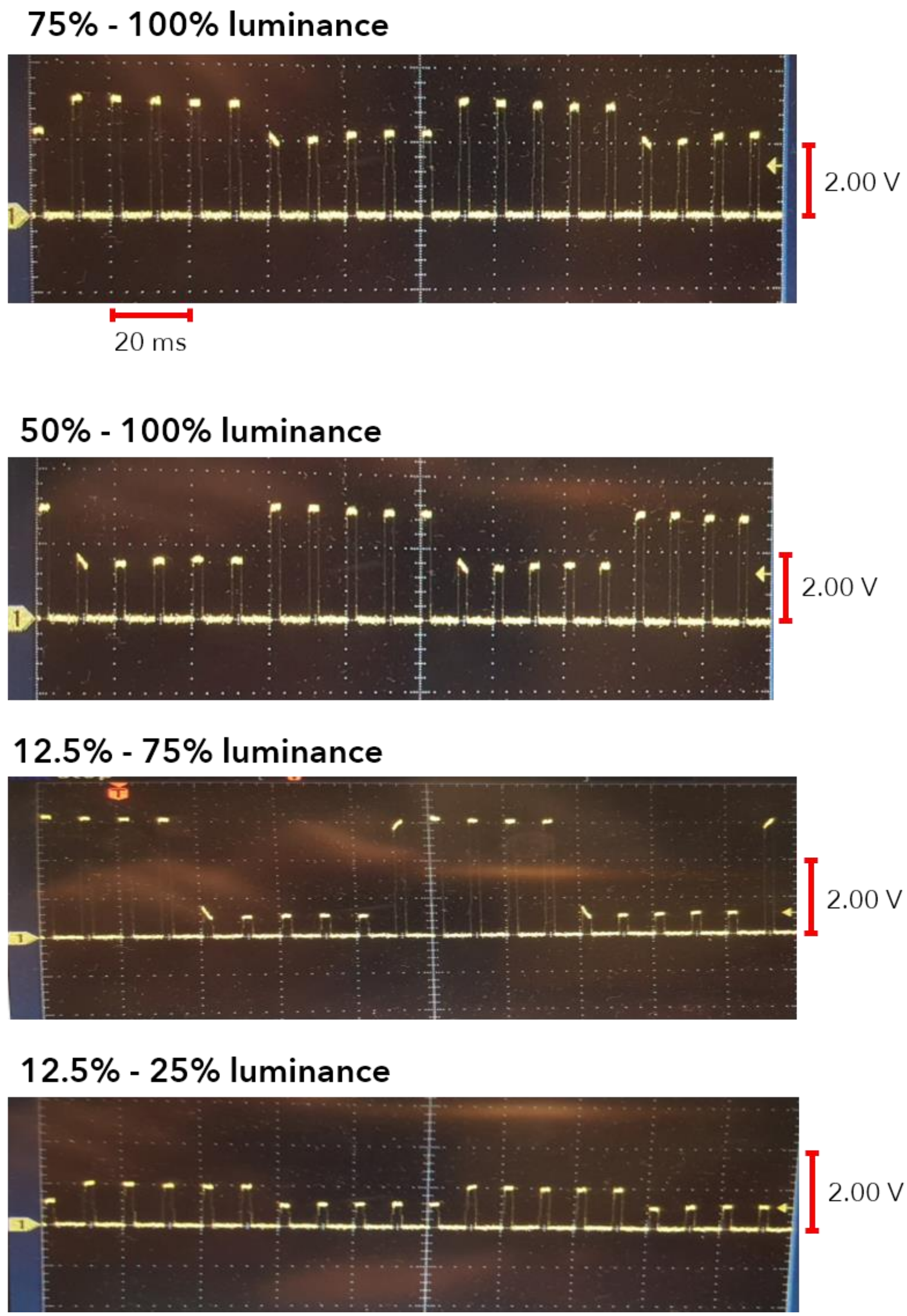

Fig. S5. Photographs of oscilloscope measurements of different luminance transitions. Luminance was changed every 5 frames while the monitor was running at 100 Hz, and with the native backlight strobing feature enabled with pulse width of 100%. The desired luminance level was reached within the first frame when the luminance was changed. For large transitions there was a small ramp within the first frame (best visible in the third panel, 12.5% - 75% luminance).

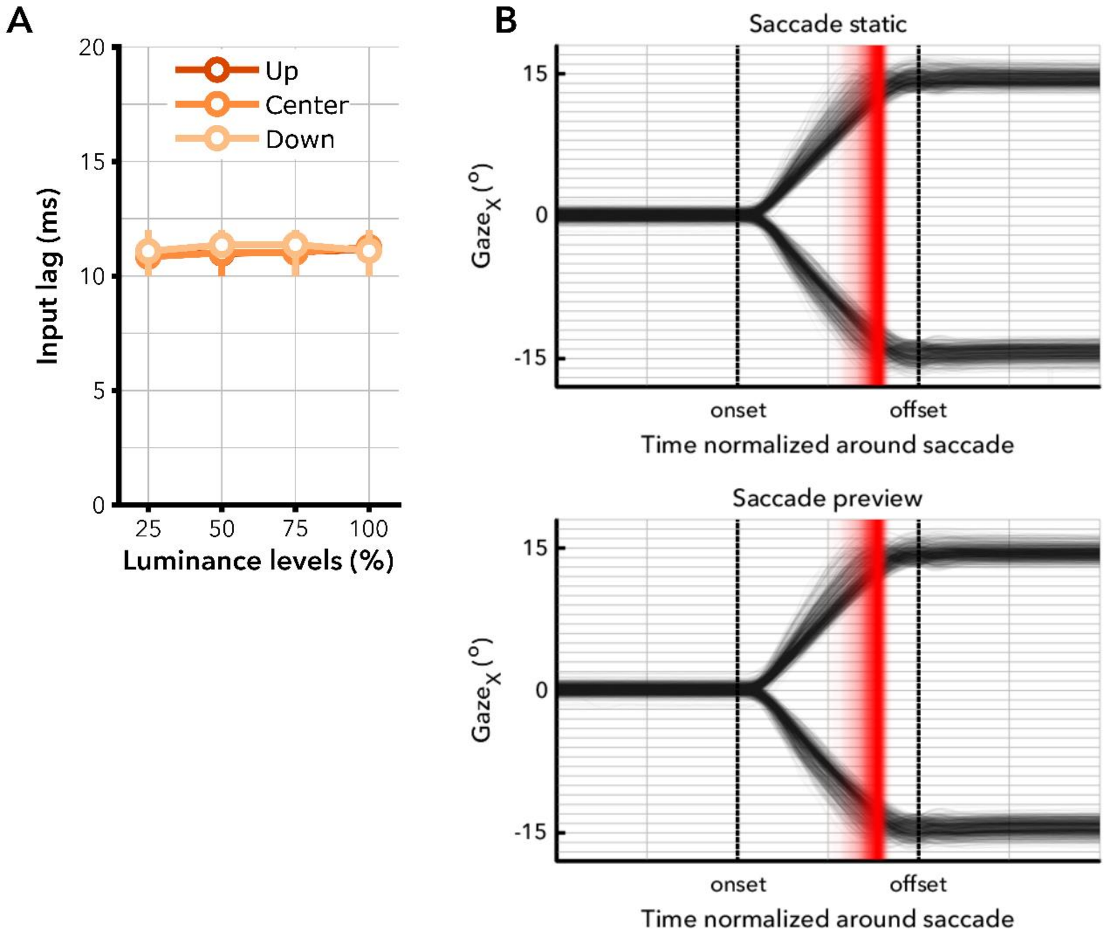

Fig. S6. Synchronization of visual onsets and timestamps in Eyelink datafile (EDF). **A)** Average input lag in ms between visual onset (as measured with a photodiode) and the timestamp in the EDF. Lags were measured at three different locations on the left side of the screen (see legend). Delays were measured from black to different luminance levels (see x-axis). Error bars represent interval including 95% measured delays. Rounded to whole milliseconds, all measured input lags were 11 ms. **B)** Horizontal gaze position over time, where time is normalized to saccade onset and offset. Red patch is the onset of the post-saccadic inducer in all trials that were included in the analysis, where the transparency reflects the density of onsets. This onset is the based on the timestamp in the EDF and corrected by 11 ms based on the photodiode measurement as displayed in A. The upper panel includes all trials from the Saccade static condition. The bottom panel includes all trials from the Saccade preview condition.

References

1. Saslow MG (1967) Effects of components of displacement-step stimuli upon latency for saccadic eye movement. *J Opt Soc Am* 57(8):1030.

2. Wandell BA (1995) A brief organized list. Available at: https://web.stanford.edu/group/vista/cgi-bin/wandell/a-brief-organized-list/.

3. Zhang GL, et al. (2018) A consumer-grade LCD monitor for precise visual stimulation. *Behav Res Methods*:1–7.